

# Electrolytic Deposition of Ni/NiO on Stainless Steel for Production of Selective Surfaces

Caio Santiago Peixoto<sup>a</sup>, Milton Teles Neto<sup>a</sup> , Yukio Shigaki<sup>a</sup>, Nilo Nogueira da Silva<sup>b</sup>,

Wagner Sade<sup>a\*</sup>

<sup>a</sup>Centro Federal de Educação Tecnológica de Minas Gerais – CEFET, Departamento de Engenharia Mecânica, Belo Horizonte, MG, Brasil

<sup>b</sup>Universidade de São Paulo – USP, Grupo de Pesquisa em Soldagem e Junções, São Paulo, SP, Brasil

Received: April 6, 2020; Revised: October 02, 2020; Accepted: November 21, 2020

The solar energy is one of the most promising energy sources today. In this context, the goal of this work is to produce selective surfaces for receiver tubes of parabolic trough collectors (PTCs). Ideally, solar collectors should have an absorbing surface that has high absorptance for radiation in the solar energy spectrum and, at the same time, low emittance. Therefore, Ni/NiO selective surfaces were produced with Ni in the first film and NiO in the second film. The method used was by electrolytic deposition of nickel on stainless steel AISI 304, followed by oxidation in a muffle furnace. The thicknesses of the coatings were measured with the photometer Digimess, making it possible to verify their variations and the surface irregularities typical of the electrodeposition procedure. The NiO film was observed in scanning electron microscope (SEM). The film hardness was evaluated by the pencil hardness test and the adhesion by the tape test.

**Keywords:** *Selective Surfaces, Concentrating Collectors, Energy, Electrolytic Deposition.*

## 1. Introduction

Currently, several studies are being carried out in the area of solar energy as a source of renewable and alternative energy. Researchers are looking for methods to achieve greater energy efficiency in the process of capturing and transforming energy from the sun's radiation.

Ideally, selective surfaces combine in high absorptance of radiation ultraviolet, visible and near infrared with low emittance in medium/distant infrared<sup>1</sup>. In 1955, at an international conference on solar energy, Tabor, Gier and Dunkle presented this idea and established the concept of selective surface and presented a first application for it<sup>2</sup>.

The optical selectivity of an absorbing surface varies due to the wavelength ( $\lambda$ ) of the incident radiation, so the selective behavior, at a given temperature, consists of absorbing all the incident radiation below a certain wavelength, known as cutoff wavelength ( $\lambda_c$ ), and do not emit radiation above this wavelength<sup>3,4</sup>. For applications in solar energy, the  $\lambda_c$  is equal to 2  $\mu\text{m}$ .

However, this  $\lambda_c$  is characteristic for different materials and types of surfaces. In the case of semiconductors, this variation is related to some properties, such as their band gap (represents the amount of energy needed for an electron to travel from the valence band to the conduction band) which is a function of the type of chemical bonds that this material presents and that will determine the amount of energy that can be absorbed<sup>5</sup>.

The microstructure of the material will also influence its  $\lambda_c$ . Materials that have impurities with a diameter smaller than the wavelength range of the incident radiation will have

their optical properties affected, because these impurities will generate multiple internal reflections to the material<sup>6</sup>.

The thickness of the selective film can also be a factor that will cause changes in  $\lambda_c$  since it can act as a filter at certain wavelengths of incident radiation and, if the thickness of the surface is high, the amount of energy emitted by radiation will also be greater<sup>7</sup>.

The efficiency of selective surfaces is commonly analyzed as a function of selectivity, a parameter defined as the ratio between absorptance in the visible range and emittance in the infrared range<sup>8</sup>.

A selective surface for photothermal purposes must have a selectivity factor greater than 5.67; but it is necessary that the solar absorptance is greater than 85% and the thermal emittance less than 15%<sup>1</sup>. When the selectivity factor is greater than 10, the surface is considered highly selective<sup>9,10</sup>. Furthermore, it must be stable at the operating temperature, have high durability and low cost.

Various methods can be used to prepare selective surfaces, such as electrolytic deposition, physical vapor deposition (PVD), chemical vapor deposition (CVD), sputtering, painting and sol-gel. Electrolytic deposition is a simple technique with a low production cost and that allows to obtain films with good properties. In addition, this deposition technique can be carried out at room temperature and atmospheric pressure, which is attractive for the industry<sup>11</sup>.

One of the challenges in the production of selective surfaces is the need for low emission, which leads to the manufacture of complex selective surfaces that are subject to degradation at the operating temperature<sup>12,13</sup>.

Thus, the goal of this work was to produce selective surfaces of Ni/NiO on stainless steel for applications in

\*e-mail: [wagnersade@hotmail.com](mailto:wagnersade@hotmail.com)

receiver tubes of parabolic trough collectors, using the process by electrolytic deposition of nickel on stainless steel, followed by oxidation in a muffle furnace.

## 2. Experimental Techniques

### 2.1 Preparation of stainless steel substrate for electrodeposition

The samples used in the depositions had as base metal the stainless steel AISI 304, with the chemical composition, by weight, presented in Table 1. This chemical composition is in accordance with the Gerdau<sup>14</sup>.

The samples were sectioned in the dimensions of 50 x 25 x 2 mm with 5 replicates per sample. The preparation of samples for the production of the selective surfaces was carried out in 2 stages: grinding in 80 and 120 sandpaper and sandblasting using a sandblasting machine.

Sandblasting was used to cause roughness in the samples and consequently increase the adhesion of depositions. In the sequence, the samples were cleaned with 99% acetone and dried with argon, according to the procedure recommended by Farooq<sup>15</sup>. After this preparation, the samples were stored in desiccators. The purpose of sample preparation was to obtain more homogeneous coatings along the substrate.

### 2.2 Electrolytic deposition of nickel on stainless steel substrates

Before electroplating, the substrates were activated in a zincate treatment aimed to increase the adhesion of the coating to the substrate. The parameters used in this treatment are shown in Table 2.

After zincate treatment, electrolytic deposition was carried out. The stainless steel electrode was used as the cathode and the nickel electrode as the anode. The DC power supply used to induce electric current was a Minipa MPL-3305M, a hot plate with magnetic stirrer was used to warm and stir the electrolyte. The parameters used in nickel

**Table 1.** Chemical composition (% w/w) of stainless steel 304 used as a substrate (Iron is left).

Elements	C	Mn	P	S	Si	N	Cr	Ni
% by weight	0.08	2.00	0.045	0.03	0.75	0.10	19.0	10.5

**Table 2.** Zincate treatment composition.

Substance	Composition
NaOH (g)	525
ZnO (g)	100
FeCl <sub>3</sub> (g)	1
C <sub>4</sub> H <sub>4</sub> KNaO <sub>6</sub> (g)	10
Deionized water (L)	0.5
Time (s)	5

**Table 3.** Electroplating parameters of nickel on stainless steel.

Substance	Electrolyte Composition	Current Density (A/dm <sup>2</sup> )	pH	Temperature (°C)
Matte Nickel	24 g of nickel sulphate, 2 g of sodium chloride, 2 g of boric acid and 100 ml of deionized water.	0.96	4.0	55

(Ni) electrodeposition are shown in Table 3, according to the Nickel Institute<sup>16</sup>. The nickel deposition time of the samples was fixed at 120 seconds for each sample.

The positioning of the samples was determined with a distance of 20 mm between the cathode and the anode in the solution and their faces were positioned in parallel with the objective of obtaining greater control over the deposition of the coatings<sup>17,18</sup>. The depositions of matte nickel on the substrate occurred along the largest area of the samples, that is, 50 x 25 cm (0.125 dm<sup>2</sup>). Several tests were made to determine the current for deposition, three values were tested, 0.12 A, 0.2 A and 1.10 A, the electrical current of 0.12 A was chosen. The purpose of working with lower currents is the search for more homogeneous coatings<sup>19</sup>. After electrolytic depositions the Ni coating thickness of the samples was measured with a Digimess TT-210 device. The measurement was made at 5 different points of the samples covered with Ni.

### 2.3 Nickel coating oxidation

The objective of oxidation was to achieve a second film of NiO. The oxidation process of the samples was carried out in a muffle furnace. Therefore, a duplex layer of Ni/NiO was obtained.

The temperature and time required for oxidation of each sample in the muffle furnace ranged between 350 to 550°C (with intervals of 50°C) for 30 minutes each<sup>20</sup>, generating J1, J2, J3, J4 and J5.

The oxidation time in the furnace set at 30 minutes (0.5 h) and the increase in temperature between the five different samples used in the process aimed to increase the amount of NiO formed. The samples were kept in the center of the furnace to increase the homogeneity of the process. The parameters used for oxidation can be seen in Table 4.

### 2.4 Characterization of the coatings

The equipment used to measure the thickness of coatings was a Digimess TT-210. The measurement was made at 5 different points of the samples covered with Ni/NiO. The oxidized film of NiO was observed at scanning electron microscope (SEM). The measures of film hardness were carried out using the pencil type instrument, Wolff Wilborn model, of the TKB Erichsen Instruments brand in accordance with ASTM D 3363<sup>21</sup>. The adhesion tests of the coating were carried out using the Tape Test based on the ASTM D 3359<sup>22</sup>.

## 3. Results and Discussion

### 3.1 Thicknesses of Ni/NiO coatings

The values obtained in the measurement of the thickness (µm) of the Ni and Ni/NiO coatings are shown in Table 5.

The thickness values of the samples increased with the temperature of the oxidation process, attesting that a

higher oxidation temperature promotes greater thicknesses. Furthermore, there were variations in relation to the measurement positions. This variation is due to the superficial heterogeneity characteristic of the electrodeposition process used to deposit the matte nickel film. The surface irregularities caused by the electrolysis method significantly influence the measuring instrument. This instrument has a relevant sensitivity to these surface irregularities, which explains the considerable values of standard deviation in measurement positions.

The variation in thicknesses between the measurement positions can also be justified by the position conditions between the anode and cathode in the electrodeposition process that causes a variation in the current density. The cathode regions (stainless steel sample) closest to the anode (pure nickel plate) have a higher current density because they are susceptible to less resistance to current flow. The more distant regions have a lower current density and this occurs, among other factors, due to small slopes of the plates that can occur in the electrodeposition process. This fact can be seen in Figure 1 where the distances between the electrodes, ideally 20 mm, vary in positions (a) and (b).

### 3.2 Morphology of samples coated with Ni

The stainless steel samples “I1”, “I2”, “I3”, “I4” and “I5” coated with nickel in the first film, that is, before the heat treatment for oxidation are shown in Figure 2. The image, in top view, shows the presence of matte nickel in the darkest areas on the surface of each sample. As the parameters for nickel deposition are the same, their morphology is similar.

### 3.3 Morphology of samples coated with Ni/NiO

Figure 3 shows the microstructures, with 1500X magnification, of stainless steel samples “J1”, “J2”, “J3”, “J4” and “J5” covered with Ni/NiO. The images were taken with a top view. The plates seen in d) and e) are due to the polarization effect originated from the use of electric current in electrolytic deposition<sup>23</sup>.

The “J1” sample, heat treated at 350°C for 30 minutes for oxidation, is shown in Figure 4 by SEM with 180X and 1500X magnification.

The samples “J2”, “J3” and “J4” coated with Ni/NiO are shown in Figure 5. The temperatures of the heat treatment of these samples were 400°C, 450°C and 500°C respectively, and each one remained in the furnace for 30 minutes. It is noted that as the oxidation temperature increases, the white

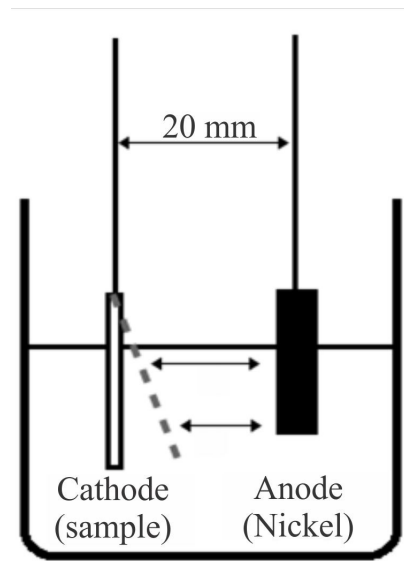
areas also increase, that is, the formation of the second film of NiO. It's important to emphasize that the oxidation time for all samples was the same, not influencing their composition.

Figure 6 shows the sample “J5” heat treated at 550°C for 30 minutes for oxidation was observed in SEM with 180X and 1500X magnification.

The formation of NiO and the presence of pores are seen in the images. However, the “J5” sample showed a higher formation of NiO (the white areas in the images) compared to the “J1” sample. This fact is notable since the oxidation temperature of the first is higher than that of the second, for the same time of 30 minutes for oxidation.

### 3.4 Pencil hardness test values

The pencil hardness test values in ascending order are shown in Table 6. Therefore, it is noted that as the amount of NiO in the coating increases, the risk hardness increases. The “J5” sample, with the highest amount of NiO, presents the greatest risk hardness and the “J1” sample, with the lowest amount of NiO, presents the lowest risk hardness. This is due to the fact that NiO is a ceramic material.



**Figure 1.** Influence of the cathode position on the thickness of the coatings.

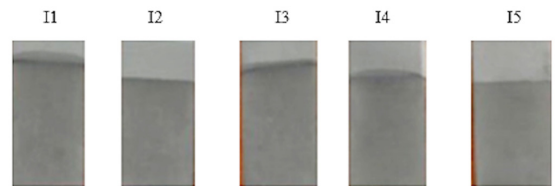


**Figure 2.** “I1”, “I2”, “I3”, “I4” and “I5” samples coated with Ni in the dark area.

**Table 4.** Time and temperature parameters for oxidation of the second film.

Sample	Time (h)	Temperature (°C)
J1	0.5	350
J2	0.5	400
J3	0.5	450
J4	0.5	500
J5	0.5	550

**Table 5.** Mean and standard deviation of the thickness of the Ni and Ni/NiO coatings.

Sample	J1	J2	J3	J4	J5
Thickness Ni (μm)	0.93 (±0.50)	0.95 (±0.60)	0.90 (±0.70)	1.00 (±0.50)	0.96 (±0.60)
Thickness Ni/NiO (μm)	1.80 (±0.90)	1.90 (±0.70)	2.20 (±1.10)	2.50 (±0.80)	3.20 (±0.50)

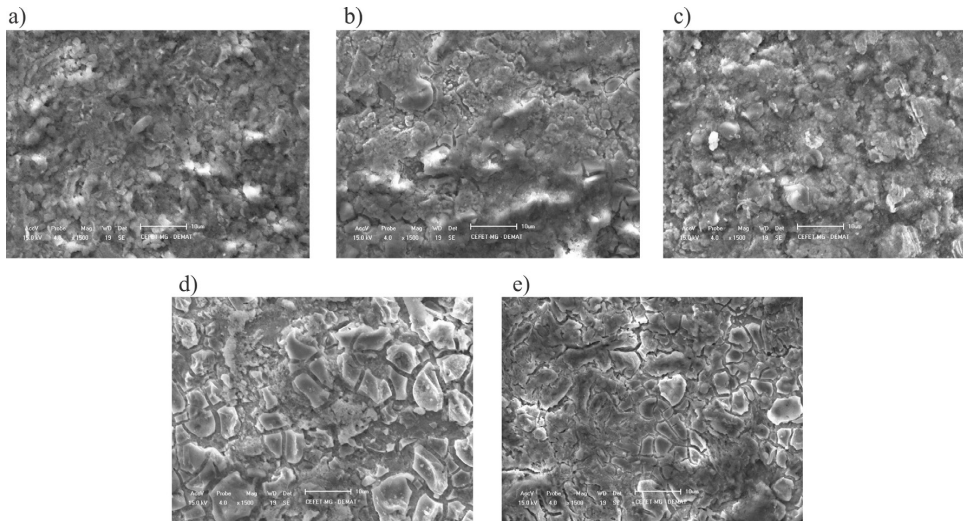


**Figure 3.** Samples coated with Ni/NiO. J1 (a), J2 (b), J3 (c), J4 (d) and J5 (e).

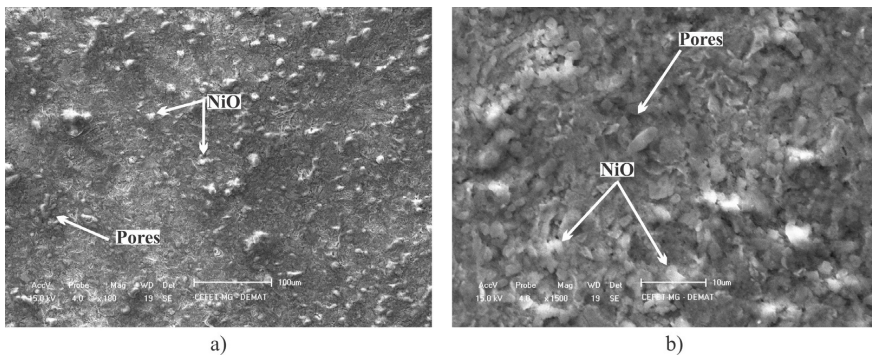


**Figure 4.** Sample "J1" coated with Ni/NiO. 180X (a) and 1500X (b).

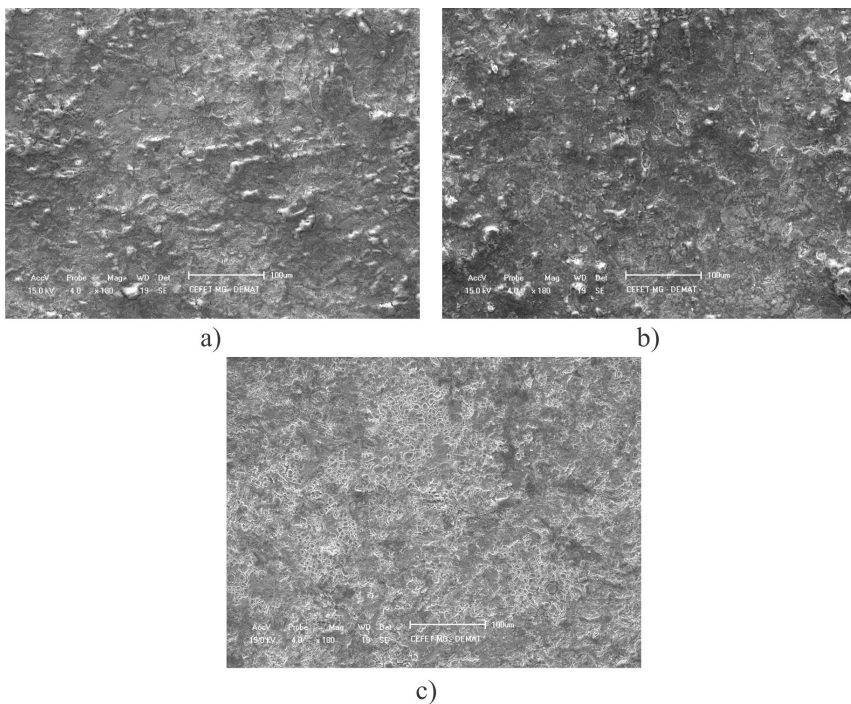


**Figure 5.** NiO coating of samples "J2" (a), "J3" (b) and "J4" (c). 1500X.

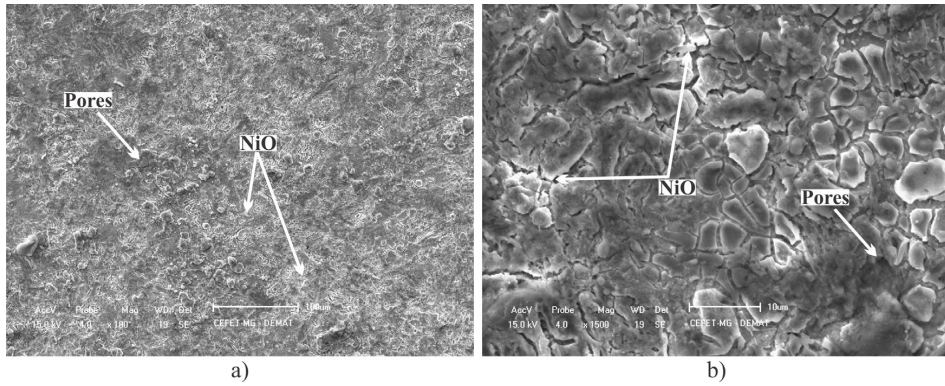


Figure 6. “J5” sample coated with Ni/NiO. 180X (a) and 1500X (b).

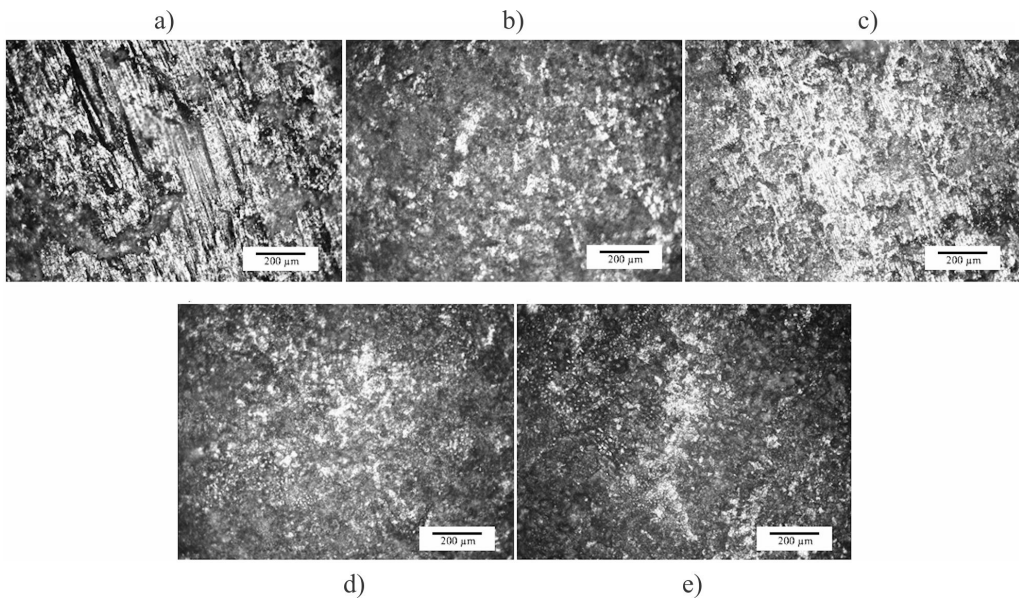


Figure 7. Adhesion tests of samples coated with Ni/NiO: J1 (a), J2 (b), J3 (c), J4 (d) and J5 (e). 200X

Table 6. Pencil hardness test results in increasing order of coatings.

Sample	J1	J2	J3	J4	J5
Film Hardness	HB	F	H	H	2H

### 3.5 The adhesion tests values

Figure 7 shows that the samples “J1” and “J3” presented less effective adhesion to the substrate, which is verified by the removal marks made by the action of the tape. However, samples “J2”, “J4” and “J5” showed a more uniform adhesion to the substrate.

Analyzing the samples “J1” and “J3” it is noted that the white areas are larger, characteristic of stainless steel substrate. The “J1” sample was oxidized at 350°C and the “J3” sample was oxidized at 400°C causing a formation of less NiO compared to the “J4” and “J5” samples oxidized at 500°C and 550°C respectively. The thicknesses of the “J1” and “J3” sample coatings are smaller than “J4” and “J5” so the loss of material in the tape adhesion test by “J1” and “J3” exposes even more the substrates.

## 4. Conclusions

The measurement of the thickness of the sample coatings showed the relation between the oxidation temperature and film thickness. Furthermore, it showed the characteristic of heterogeneity caused by the use of electrodeposition. The irregularities of the surfaces created by the procedure caused variations in the measurements of the thickness of the films.

The morphological analysis carried out by the images generated by the Scanning Electron Microscope (SEM), showed the Ni/NiO structure for all five samples produced.

The “J5” sample submitted to a temperature of 550°C achieved greater oxidation than the “J1” sample submitted to 350°C, this fact was observed by SEM. In other images generated by SEM of the samples produced, “J2”, “J3” and “J4”, the oxidation gradation of the coating in the samples was verified, thus obtaining the expected result.

The film hardness test evaluated the hardness of the produced surfaces that varied between HB (sample J1), H (samples J2 and J4), F (sample J3) and 2H (sample J5).

The Tape Test generated a qualitative analysis of the adhesion of the coating to the substrate, showing that samples

J1 and J3 presented less adhesion to the substrate than the other samples analyzed (J2, J4 and J5).

Therefore, the definition of the procedures carried out in this electrodeposition work allowed to achieve the most adequate results about the nickel coating. From the variation of the electric current and fixation of the electrodeposition time (120 seconds) it was confirmed that the current of 0.12 A presented a better deposited film.

## 5. References

1. Nunes RAX, Costa VC, Sade W, Araújo FR, Silva GM. Selective surfaces of black chromium for use in solar absorbers. *Mater Res*. 2017;21(1):1-5.
2. Nahar NM, Mo GH, Ignatiev A. Development of an Al<sub>2</sub>O<sub>3</sub>-Co selective absorber for solar collectors. *Thin Solid Films*. 1989;172:19-25.
3. Amri A, Duan XF, Yin C-Y, Jiang Z-T, Rahman MM, Pryor T. Solar absorptance of copper-cobalt oxide thin film coating with nano-size, grain-like morphology: Optimization and synchrotron radiation XPS studies. *Appl Surf Sci*. 2013;275:127-35.
4. Madhukeshwara N, Prakash ES. An investigation on the performance characteristics of solar flat plate collector with diferente selective surface coatings. *Int J Energy Environ*. 2012;3:99-108.
5. Callister WD. *Ciência e engenharia de materiais*. Rio de Janeiro: LTC; 2008.
6. Martins M. *Produção de superfícies seletivas por magnetron sputtering para aplicação em coletores solares [dissertation]*. Rio de Janeiro: Universidade Federal do Rio de Janeiro; 2010.
7. Rebouta L, Pitães A, Andritschky M, Capela P, Cerqueira MF, Matilainen A, Pischow K. Optical characterization of TiAlN/TiAlON/SiO<sub>2</sub> absorber for solar selective applications. *Surf Coat Tech*. 2012;211:41-4.
8. Kennedy CE. *Review of mid-to-high temperature solar selective absorber materials*. Colorado: National Renewable Energy Laboratory; 2002.
9. Krenzinger A. *Superfícies seletivas para conversão térmica da energia solar, óxido de cobre sobre cobre [dissertation]*. Porto Alegre: Universidade Federal do Rio Grande do Sul; 1979.
10. Xiao X, Miao L, Xu G, Lu L, Su Z, Wang N, Tanemura S. A facile process to prepare copper oxide thin films as solar selective absorbers. *Appl Surf Sci*. 2011;257(24):10729-36.
11. Medeiros IDM, Gonçalves RPN, Menezes VL, Galvão GO, Gomes KC. Evaluation of potential residual silica as antireflective layer for selective solar surface of black chromium. *Mater Res*. 2019;22(3):1-6.
12. Mihelcic M, Francetič V, Kovač J, Šurc Vuk A, Orel B, Kunič R, Peros D. Novel sol-gel based selective coatings: from coil absorber coating to high power coating. *Sol Energy Mater Sol Cells*. 2015;140:232-48.
13. Zheng L. Optical design and co-sputtering preparation of high performance Mo-SiO<sub>2</sub> cermet solar selective absorbing coating. *Appl Surf Sci*. 2013;280:240-6.
14. Gerda. *Manual de aços [homepage on the Internet]; 2007 [cited 2019 Oct 18]*. Available from: [https://www.feis.unesp.br/Home/departamentos/engenhariamecanica/maprotec/catalogo\\_acos\\_gerda.pdf](https://www.feis.unesp.br/Home/departamentos/engenhariamecanica/maprotec/catalogo_acos_gerda.pdf)
15. Farooq M, Raja IA. Optimization of metal sputtered and electroplated substrates for solar selective coating. *Renewable Energy*. 2008;33:1275-1285.
16. Nickel Institute. *Nickel plating handbook*. Belgium: Nickel Institute: Knowledge for a Brighter Future; 2014.
17. Peixoto CS, Xavier Nunes, RA, Sade, W. *Deposição eletrolítica de níquel seguido de oxidação para aplicações em concentradores solares*. In: *I Simpósio de Engenharia de Materiais do CEFET-MG*; 2018 Sep 12-14; Belo Horizonte, MG.
18. Lira-Cantú M, Sabio AM, Brustenga A, Gómez-Romero P. Electrochemical deposition of black nickel solar absorber coatings on stainless steel AISI316L for thermal solar cells. *Sol Energy Mater Sol Cells*. 2004;87:685-94.
19. Teixeira R. *Recobrimento seletivo nanoestruturado para coletores solares de base níquel obtido sobre substrato de cobre por técnicas eletroquímicas [thesis]*. Rio de Janeiro: Universidade Federal do Rio de Janeiro; 2011.
20. Sade W, Nunes RAX, Branco JRT. *Produção de superfícies seletivas de Ni/NiO por processos químico e eletrolítico em substrato de alumínio*. *Rev. Esc. Minas*. 2009;62(3):361-5.
21. ASTM: American Society for Testing and Materials. *ASTM D 3363: Standard test method for film hardness by pencil test*. West Conshohocken: ASTM; 2005.
22. ASTM: American Society for Testing and Materials. *ASTM D 3359: Standard test methods for measuring adhesion by tape test*. West Conshohocken: ASTM; 2004.
23. Sade W. *Produção de superfícies seletivas de Ni/NiO para aplicações em coletores solares [thesis]*. Belo Horizonte: REDEMAT; 2011.